Low-energy valence photoemission in Ce compounds: Beyond the Anderson impurity model

J. D. Lee
Max-Planck Institut für Festkörperforschung, Heisenbergstrasse 1, D-70569 Stuttgart, Germany
(Received 7 July 1999)

The valence level photoemission spectra in the Anderson impurity model for Ce compounds at zero temperature are studied as a function of the photon energy ω. Most of the former studies on Ce compounds are based on the sudden approximation, which is valid in the high energy region. For the photoemission in the adiabatic limit of the low-energy region, one should consider the dipole matrix elements and the dynamic photoelectron scattering potential. We can manage it by combining the time-evolution formalism and the $1/N_f$ scheme in a large f-level degeneracy N_f. This gives the exact results as $N_f \to \infty$. In view of experiments on the valence photoemission, two contributions of $4f$ and band emissions are mixed. We study the separate $4f$ and band contributions (from Ce $5d$) and total emission including the interference between two on an equal footing with varying the photon energy. In the $4f$-emission case, we also explore the effects of dynamic scattering potential of the photoelectron with respect to ω, for which the extended model is proposed. Its effects are found very similar to the core level photoemission in the shake down case with a localized charge transfer excitation. Additionally, we examine the adiabatic-sudden transition in valence level photoemission for the present localized system through the simplified two-level model.

I. INTRODUCTION

The Anderson impurity model (AIM) was originally proposed to discuss the property of magnetic impurities in nonmagnetic metals.[1] After that, AIM has been widely applied to the analysis of spectroscopic data for f and d electron systems, i.e., rare earth compounds[2] or transition metal compounds,[3] where electron states are treated to be an impurity and they are hybridized with the valence or conduction electron states. Also, AIM has been often used to describe the Ce mixed-valence compounds, where one considers the f level on one atom and its interaction with the conduction bands. In investigations of Ce and its compounds, the basic question concerns the nature of a $4f$ electron and other electronic states and how they mix with the $4f$ state. Much of the interests are therefore imposed on the properties of the $4f$ states, i.e., the occupation, position, width, coupling to the metallic band, intra-atomic Coulomb interaction, and so on. There were numerous studies of thermodynamic and transport properties for them, which has been followed by the electron-spectroscopy studies.[4]

The photoemission spectroscopy (PES) is a very useful tool for studying the electronic structure of matters and could have provided a lot of insights also for Ce studies. But it is worth noting PES cannot always give a simple answer about the underlying electronic structure because the photoelectron may perturb the system left behind. An actual description of theoretical PES is quite complicated and therefore the sudden approximation is frequently used, where the photoelectron is assumed decoupled from the remaining solid.[5] The sudden approximation becomes exact when the kinetic energy of the emitted electron gets large infinitely.

Gunnarsson and Schönhammer[6] have extensively studied the electron spectroscopies for Ce compounds, i.e., core level photoemission, x-ray absorption, and bremsstrahlung isochromat spectroscopy as well as the valence photoemission. For the information of the position and width of f level in the compounds, the valence photoemission has often been used. Through their studies of valence photoemission in f-emission channel, they reproduced two-peak structure in Ce compound using AIM consistent with the experiments. In the earlier evolution stage for Ce materials, it was found that the valence PES shows just a single f-related structure 2–3 eV below the Fermi level.[7,8] Later PES experiments have demonstrated the $4f$ spectrum has the additional structure interestingly near the Fermi level.[9–12] Subsequently, it was shown that the particular structure is due to the Kondo resonance singlet characterized by the small energy T_K. In the actual experiments on valence photoemission, two contributions of $4f$ emission and band emission (from Ce $5d$ or other bands) are mixed. The identification of $4f$ emission from the experiments is a highly nontrivial work. Wieliczka *et al.*[11] have reported the additional peak near the Fermi level using the resonant $4f$ emission. Another possibility is to assume the behaviors of $4f$ and band emissions with respect to the photon energies, especially in 20–80 eV.[13] Nevertheless, they could have said nothing about the interference between the two. These works can motivate to explore a more explicit analysis for the interference effects of two emission channels with the photon energy varied. Gunnarsson and Schönhammer[14] have also studied the band emission contribution as well as $4f$ emission and discussed the interference effects of the two. However, all their works were within the sudden approximation.

We consider both the contributions of $4f$ and $5d$ emission on an equal footing by introducing two dipole matrix elements $\Delta_f(E)$ and $\Delta_d(\epsilon,E)$, where E is the kinetic energy of photoelectrons. In the sudden approximation, the dipole matrix elements are normally treated constant with E. But in the low energy PES, it can be crucial. Combining the time-dependent formalism and $1/N_f$ idea, we can calculate the PES exactly up to $\mathcal{O}(1/N_f)^0$ as the photon energy varies. $N_f=\infty$ can be a good approximation to $N_f=14$ in Ce compounds. Then we study the separate contributions of $4f$ and

 ©2000 The American Physical Society

$5d$ emission and more interestingly the nontrivial interference effects between the two. The relative sign or strength of $\Delta_f(E)$ and $\Delta_d(\epsilon,E)$ are important. Difference in the energy scale of $\Delta_f(E)$ and $\Delta_d(\epsilon,E)$ makes the spectra from each channel separate with respect to ω in the low energy PES. It is also found that, because the interference contribution has a peak near the Fermi level, the $4f$-derived peak near the Fermi level may be enhanced or suppressed in the total spectra.

It has recently been reported that the adiabatic-sudden transition due to the photoelectron scattering potential will be governed by the characteristic of relevant excitations to which the emitted electron couples in the system. When the photoelectron couples to the extended excitation like plasmon, the sudden transition occurs in very large kinetic energies ($\sim$keV),[15] while to the localized excitations, the sudden approximation occurs much quicker.[16] In our study, the extrinsic effects with respect to ω beyond the sudden approximation will be considered only through the extended impurity model including the dynamic hole-induced scattering potential. Effects such as surface or several damping mechanisms will not be taken into account. The recent angle-resolved photoemission spectra (ARPES) in Ce or other *f*-electron systems shows that another notable feature in the low energy spectra is its angle dependent modulation,[17] which is thought of as the lattice effects of the *f* level and should be understood from the Anderson lattice model. Nevertheless, the merit of AIM is that the *f*-emission spectra integrated over **k** is closely approximated by the impurity *f*-spectral function.[18,19] The system of Ce compounds has also included the localized excitations represented by f^0, f^1, f^2 created from the hole potential. We can consider the scattering potential in the valence PES due to the *f* hole in the impurity model within the formalism. The scattering effects will not be important for band emission channel. The crossover from adiabatic to sudden limit can be also reexamined in this localized system, for which we simplify the model to have only two relevant levels. The same criterion for the transition is found as in the previous work,[16] the energy scale of $\tilde{E}=1/(2\tilde{R}^2)$, where $\tilde{R}$ is a scattering potential range.

We organize the paper as follows. Our model and the formalism for calculation are given in Sec. II. The simple sudden approximation results for separate and both channels are described in Sec. III. In Sec. IV, we present the model for necessary dipole matrix elements and calculate the spectra for the separate contributions for $4f$ and $5d$ emission and for both with respect to the photon energies. We also discuss the interference contribution between two. In Sec. V, for $4f$ emission, we extend the model to include the photoelectron scattering potential and study its effects within the same formalism. In Sec. VI, we try to reexamine the adiabatic-sudden crossover in the system by way of the simplified two-level model. In Sec. VII, we give the discussion and conclusion.

II. MODEL AND FORMALISM

As mentioned in the Introduction, we consider the AIM Hamiltonian in the energy basis used in Gunnarsson and Schönhammer's discussion for Ce compounds,[6,14]

$$\mathcal{H}=\mathcal{H}_0+\Delta,$$

$$\mathcal{H}_0=\sum_\nu \int E\psi^\dagger_{E\nu}\psi_{E\nu}dE+\sum_\nu \int \epsilon\psi^\dagger_{\epsilon\nu}\psi_{\epsilon\nu}d\epsilon+\epsilon_f\sum_\nu n_\nu$$
$$+\sum_\nu \int V(\epsilon)(\psi^\dagger_\nu\psi_{\epsilon\nu}+\psi^\dagger_{\epsilon\nu}\psi_\nu)d\epsilon+\frac{U}{2}\sum_{\nu\neq\nu'} n_\nu n_{\nu'}, \tag{1}$$

where $\psi^\dagger_{E\nu}(\psi_{E\nu})$ is a photoelectron operator, ϵ denotes the $5d$ conduction states, ϵ_f describes the impurity $4f$ level, and $V(\epsilon)$ is a hybridization matrix element between the conduction states and localized *f* level. $|V(\epsilon)|^2$ can be modelized to have a semielliptical form symmetric with respect to $\epsilon_F=0$, $\pi|V(\epsilon)|^2=2V^2(B^2-\epsilon^2)^{1/2}/B^2$, where $2B$ is the bandwidth. Δ in the Hamiltonian is the dipole term describing the photon-matter interaction. The one particle basis used in Eq. (1) is introduced by assuming[20]

$$\sum_{\mathbf{k}} V^*_{\mathbf{k}m}V_{\mathbf{k}m'}=|V(\epsilon)|^2\delta_{mm'},$$

$$\psi^\dagger_{\epsilon\nu}=V(\epsilon)^{-1}\sum_{\mathbf{k}} V^*_{\mathbf{k}m}\delta(\epsilon-\epsilon_{\mathbf{k}})\psi^\dagger_{\mathbf{k}\sigma},$$

and so ν is the orbital and spin magnetic quantum number and from $\nu=1$ to $\nu=N_f$ if we assume the magnetic degeneracy N_f of *f*-level. In Ce, N_f is normally taken as 14. To apply $1/N_f$ idea, we need one subsidiary condition that $N_f^{1/2}V(\epsilon)$ should be independent of N_f.

In Δ, we will generally have two interaction terms due to $4f$ level and $5d$ conduction bands, so

$$\Delta=\sum_\nu \int dE[\Delta_f(E)\psi^\dagger_{E\nu}\psi_\nu+\Delta^*_f(E)\psi^\dagger_\nu\psi_{E\nu}]$$
$$+\frac{1}{N_f^{1/2}}\sum_\nu \int d\epsilon dE[\Delta_d(\epsilon,E)\psi^\dagger_{E\nu}\psi_{\epsilon\nu}$$
$$+\Delta^*_d(\epsilon,E)\psi^\dagger_{\epsilon\nu}\psi_{E\nu}]. \tag{2}$$

By giving the explicit time dependency $f(\tau)$ in Δ and redefining the dipole matrix elements, $\Delta_f(E)$ and $\Delta_d(\epsilon,E)$,

$$\Delta_f(E)\rightarrow M_f\Delta_f(E)f(\tau),$$
$$\Delta_d(\epsilon,E)\rightarrow M_d\Delta_d(\epsilon,E)f(\tau), \tag{3}$$
$$f(\tau)=e^{-i\omega\tau}(e^{-\eta\tau}-1),\quad \eta>0 \tag{4}$$

we use a time-dependent formulation and solve the Schrödinger equation for the total Hamiltonian $\mathcal{H}$.

We first introduce a state $|0\rangle$,

$$|0\rangle=\prod_\nu^{N_f}\prod_{\epsilon<\epsilon_F}\psi^\dagger_{\epsilon\nu}|\text{vac}\rangle, \tag{5}$$

where all the conduction electron states below Fermi energy are occupied and the *f* level is empty. For the simplicity, we keep only the lowest order terms of $1/N_f$ before and after the photoemission, which means the results will be exact as $N_f\rightarrow\infty$:

$$|\epsilon\rangle = \frac{1}{N_f^{1/2}} \sum_{\nu} \psi_{\nu}^{\dagger}\psi_{\epsilon\nu}|0\rangle, \tag{6}$$

$$|\epsilon,\epsilon'\rangle = \frac{1}{N_f^{1/2}(N_f-1)^{1/2}} \sum_{\nu\neq\nu'} \psi_{\nu}^{\dagger}\psi_{\nu'}^{\dagger}\psi_{\epsilon'\nu'}\psi_{\epsilon\nu}|0\rangle, \tag{7}$$

$$|E,\epsilon\rangle = \frac{1}{N_f^{1/2}} \sum_{\nu} \psi_{E\nu}^{\dagger}\psi_{\epsilon\nu}|0\rangle, \tag{8}$$

$$|E,\epsilon,\epsilon'\rangle = \frac{1}{N_f^{1/2}(N_f-1)^{1/2}} \sum_{\nu\neq\nu'} \psi_{E\nu}^{\dagger}\psi_{\nu'}^{\dagger}\psi_{\epsilon'\nu'}\psi_{\epsilon\nu}|0\rangle, \tag{9}$$

$$|E,\epsilon,\epsilon',\epsilon''\rangle = \frac{1}{N_f^{1/2}(N_f-1)^{1/2}(N_f-2)^{1/2}} \times \sum_{\nu\neq\nu'\neq\nu''} \psi_{E\nu}^{\dagger}\psi_{\nu'}^{\dagger}\psi_{\nu''}^{\dagger}\psi_{\epsilon''\nu''}\psi_{\epsilon'\nu'}\psi_{\epsilon\nu}|0\rangle. \tag{10}$$

Within the above basis set, after time τ, the wave function $|\Psi(\tau)\rangle$ of the system is given by

$$\begin{aligned}|\Psi(\tau)\rangle = a(\tau)|0\rangle &+ \int b(\epsilon;\tau)|\epsilon\rangle d\epsilon \\ &+ \int c(\epsilon,\epsilon';\tau)|\epsilon,\epsilon'\rangle d\epsilon d\epsilon' \\ &+ \int d(E,\epsilon;\tau)|E,\epsilon\rangle dE d\epsilon \\ &+ \int e(E,\epsilon,\epsilon';\tau)|E,\epsilon,\epsilon'\rangle dE d\epsilon d\epsilon' \\ &+ \int f(E,\epsilon,\epsilon',\epsilon'';\tau)|E,\epsilon,\epsilon',\epsilon''\rangle dE d\epsilon d\epsilon' d\epsilon''.\end{aligned} \tag{11}$$

The coefficients of $|\Psi(\tau)\rangle$ can be determined by the time-dependent Schrödinger equation

$$i\frac{\partial}{\partial\tau}|\Psi(\tau)\rangle = \mathcal{H}|\Psi(\tau)\rangle, \tag{12}$$

where the initial condition of the state should be corresponding to the ground state before the photoemission $|\Psi(\tau=0)\rangle = |\Psi_0\rangle$

$$\begin{aligned}|\Psi(0)\rangle = a(0)|0\rangle &+ \int b(\epsilon;0)|\epsilon\rangle d\epsilon \\ &+ \int c(\epsilon,\epsilon';0)|\epsilon,\epsilon'\rangle d\epsilon d\epsilon'\end{aligned} \tag{13}$$

and the equations for $a(0)$, $b(\epsilon;0)$, and $c(\epsilon,\epsilon';0)$ are found in Ref. 14. The coefficients M_f and M_d represent the external field strength. In the present formalism, we solve the equation in the limit of $M_f \to 0$ and $M_d \to 0$ and let the system evolve for a time of the order $1/\eta$. Then we can show the solution identical to the more conventional photoemission.[16,21] η is a small positive number and gives a lifetime broadening in the spectra. In the actual calculation, η is taken as 0.3 eV (0.01 a.u.). The photoemission spectra will now be proportional to

$$\begin{aligned}I(E) = &\int |d(E,\epsilon;\tau)|^2 d\epsilon + \int |e(E,\epsilon,\epsilon';\tau)|^2 d\epsilon d\epsilon' \\ &+ \int |f(E,\epsilon,\epsilon',\epsilon'';\tau)|^2 d\epsilon d\epsilon' d\epsilon'',\end{aligned} \tag{14}$$

and we see, due to $M_f \to 0$ and $M_d \to 0$,

$$I(E) = \alpha(E)M_f^2 + \beta(E)M_d^2 + \gamma(E)M_f M_d, \tag{15}$$

where $\alpha(E)$, $\beta(E)$, and $\gamma(E)$ correspond to $4f$, $5d$ emission, and interference between those, respectively.

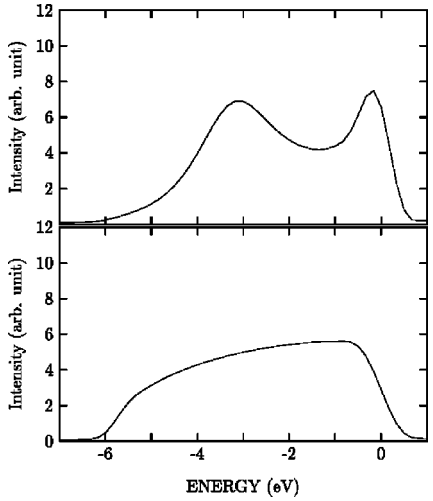

FIG. 1. In the upper panel, the f-derived valence PES is provided ($M_d = 0$) and in the lower panel, the conduction band emission is given ($M_f = 0$) for $U = 5.0$ eV, $\epsilon_f = -2.5$ eV, $V = 0.5$ eV, and $B = 6$ eV. Both calculations are based on the sudden approximation. Spectral curves are normalized to have the same area.

III. SUDDEN APPROXIMATION

In the sudden approximation, we normally neglect E dependency of the dipole matrix elements, i.e., $\Delta_f(E) = M_f$ and $\Delta_d(\epsilon,E) = M_d\Delta_d'(\epsilon)$, where E is a kinetic energy of photoelectron. Gunnarsson and Schönhammer[14] assumed $\Delta_d'(\epsilon)$ have the same shape as $V(\epsilon)$ for the conduction band emission, which we will simply follow.

The AIM has often been studied in the limit of $U = \infty$, where it becomes so simple as to allow the analytic solutions. In our formalism, to neglect $|\epsilon,\epsilon'\rangle$ and $|E,\epsilon,\epsilon',\epsilon''\rangle$ corresponds to the limit. However the assumption $U = \infty$ is not really justified because U is just about 5–6 eV (Ref. 22) and thus f^0 and f^2 configurations are energetically comparable, i.e., ϵ_f is about -2–-3 eV (Ref. 7) and $2\epsilon_f + U \approx 0$. In the calculations, we have always taken $U = 5.0$ eV and $\epsilon_f = -2.5$ eV to be $2\epsilon_f + U = 0$. In Fig. 1, we give the simple valence PES results for $4f$ and $5d$ emission, respectively.

It is seen in Fig. 1 that we nicely reproduce the well-

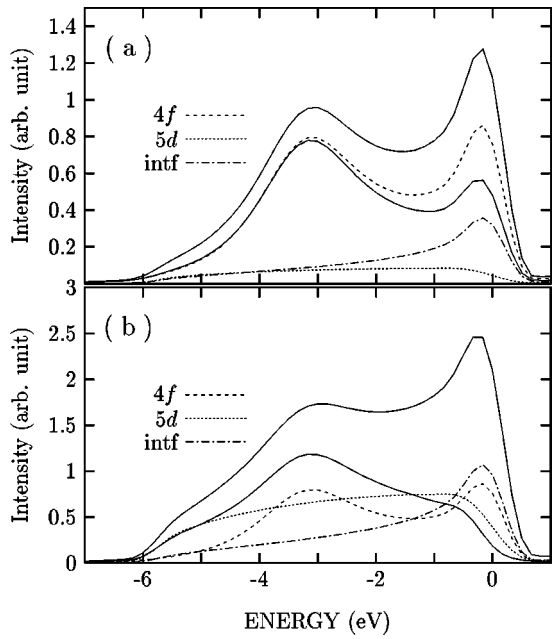

FIG. 2. The valence PES including both contributions of $4f$ and $5d$ emission is shown. Two solid lines are the total spectra corresponding to constructive or destructive interference, where interference effects (labeled intf) is added or subtracted. In (a), we use $|\tilde{\Delta}_d/\tilde{\Delta}_f|=2.0$ and in (b), $|\tilde{\Delta}_d/\tilde{\Delta}_f|=6.0$. The used parameters are same in Fig. 1.

known sudden $4f$-PES results[14] having the double-peak structure in the upper panel and also get $5d$ PES simulating the broad structureless conduction band. The $4f$ PES is especially interesting because of its ample physics. The peak well below the Fermi level corresponds to $4f$ ionization peak, $4f^1 \rightarrow 4f^0$, and the peak near the Fermi level (also called Kondo resonance peak) arise from a $4f$ hole screened by a $4f$ electron (making a $5d$ hole near the Fermi level), $4f^1 \rightarrow 4f^1$.

In the separate calculations of emission channels, the absolute values or signs of M_f and M_d are surely irrelevant to the results. There can be, however, some subtleties when we consider both emission channels. The PES curves drastically change with respect to the relative sign or relative ratio of M_f and M_d. For the relative strength, we parametrize the ratio of $|\tilde{\Delta}_d/\tilde{\Delta}_f|$, where $\tilde{\Delta}_d \equiv M_d \Delta'(0)$ and $\tilde{\Delta}_f \equiv M_f$ (note $|\tilde{\Delta}_d/\tilde{\Delta}_f|>1$ does not always mean the band emission is dominant over the f emission). The relative sign is related to whether the interference will be constructive or destructive.

As shown in Fig. 2, the relative ratio and sign of two dipole components are crucial in valence PES. Interestingly, the interference contributions show a peak near the Fermi level, which may enhance the Kondo resonance peak from $4f$ emission in the constructive case or suppress in the destructive case. In Fig. 2(b), in the total spectra, even if we can see a clear ionization peak near ϵ_f, we see only the shoulder structure not a peak near the Fermi level due to a strong destructive interference.

IV. LOW ENERGY VALENCE PHOTOEMISSION: EFFECTS OF DIPOLE MATRIX

In the last section, we have illustrated the sudden approximation results valid in the high-energy PES. To see how the PES behaves in the low-energy regime, first off we should account for the E-dependent dipole matrix elements. Using the *Slater-type* orbital[23] for the corresponding atomic orbital, we calculate E-dependent dipole matrix elements. The Slater orbital for $R_{nl}(r)$ is given by

$$R_{nl}(r)=(2\zeta)^{n+1/2}[(2n)!]^{-1/2} r^{n-1} e^{-\zeta r}, \tag{16}$$

where the orbital exponent is determined by a suitable rule. But in the $4f^1 5d^1 6s^2$ configuration of Ce, the Slater orbital for $5d$ gives actually the poor representation compared to a more accurate LSD calculation[24] for the atomic wave function for Ce. We adopt therefore the same functional form of Eq. (16), but determine the exponent ζ suitably by comparing with the accurate result, i.e., we take $\zeta_{4f}=5.0$ and $\zeta_{5d}=2.0$ (by a Slater-rule, ζ_{5d} will be 0.75). In principle, the atomic orbital and photoelectron basis function having an explicit angular momentum channel l should be obtained by solving the Schrödinger equation under the same Ce atomic potential. But in our discussion the basis function is simply assumed to be a spherical Bessel function of l,

$$\varphi_E^l(r)=\frac{\sqrt{2}}{\sqrt{\pi}}(2E)^{1/4} j_l(\sqrt{2E}r), \tag{17}$$

and its normalization follows

$$\int r^2 dr\, \varphi_E^l{}^*(r)\varphi_{E'}^l(r)=\delta(E-E'). \tag{18}$$

So the dipole matrix elements for $4f$ emission is given by

$$\Delta_f(E)=M_f \int r^2 dr R_{4f}(r) r \varphi_E^{l=4}(r), \tag{19}$$

and for the $5d$-conduction band emission, we assume $\Delta_d(\epsilon,E)$ has a simple separable form similar to

$$\Delta_d(\epsilon,E)=M_d \Delta_d'(\epsilon)\Delta_d(E). \tag{20}$$

$\Delta_d'(\epsilon)$ is still assumed to have the shape of $V(\epsilon)$ as in the last section and $\Delta_d(E)$ can be expected to have much $5d$ atomic orbital character if we think of the tight binding idea for the corresponding energy band. Thus we assume the behavior of $\Delta_d(E)$ as

$$\Delta_d(E) \propto \int r^2 dr R_{5d}(r) r \varphi_E^{l=3}(r). \tag{21}$$

Here it should be noted that the possible l-channel of photoelectrons are $l=2,4$ for $4f$-emission and $l=1,3$ for $5d$ emission due to the angular momentum selection rule, but the major channel will be $l=4$ and $l=3$, respectively.

In Fig. 3, we give the dipole matrix behaviors of $\Delta_f(E)$ and $\Delta_d(E)$. This is obtained from very crude calculations, but qualitatively quite consistent with the calculation of Yeh and Lindau[25] of photoionization cross sections for Ce. We can simply expect from the behaviors of dipole elements the general trend is that in the low energy, d emission will be dominant over f emission, while in the high energy, f emission dominant over d emission. We first show the calculation result for separate $4f$ and $5d$ contributions with respect to various photon energies ω.

Figure 4 shows ω-dependent $4f$ and $5d$ emission, the

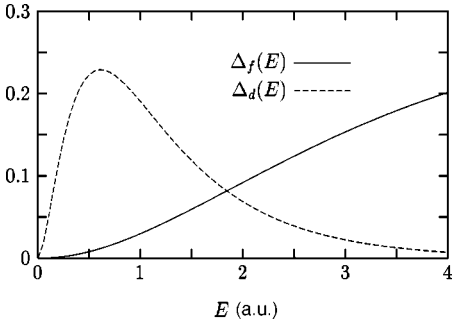

FIG. 3. The behaviors of dipole matrix elements-$\Delta_f(E)$, $\Delta_d(E)$ are provided with respect to the photoelectron kinetic energy E. Note the different energy scale in two behaviors. The absolute values are arbitrary.

changes of spectral weight and shape with ω varied. The spectral weight will be proportional to the square of dipole matrix elements at the corresponding energies and the shape related to the behaviors of dipole element. If the $5d$ radial wave function does not vary significantly for La and Ce, the bottom panel of the figure can be compared with the PES for La (Ref. 11) and found to be consistent with the experiment. We can also find as ω increases the spectral shape approaches the sudden approximation results (see the insets).

Now we investigate the total valence PES to which both $4f$ and $5d$ emission contribute with respect to various photon energies ω. To parametrize the relative strength of two dipole matrix effects, we redefine $\tilde{\Delta}_f$ and $\tilde{\Delta}_d$ as $\tilde{\Delta}_f \equiv \Delta_f(E)|_{E=4.0}$, $\tilde{\Delta}_d \equiv \max\{\Delta_d(\epsilon,E)\}$. That is, $\tilde{\Delta}_f$ is defined as the value of $\Delta_f(E)$ at $E=4.0$ and $\tilde{\Delta}_d$ as the value of $\Delta_d(\epsilon,E)$ at $\epsilon=0.0$ and $E\approx 0.6$ (see Fig. 3). We give the behaviors of valence PES as ω varied for $|\tilde{\Delta}_d/\tilde{\Delta}_f|=2.0$ and $|\tilde{\Delta}_d/\tilde{\Delta}_f|=6.0$, respectively.

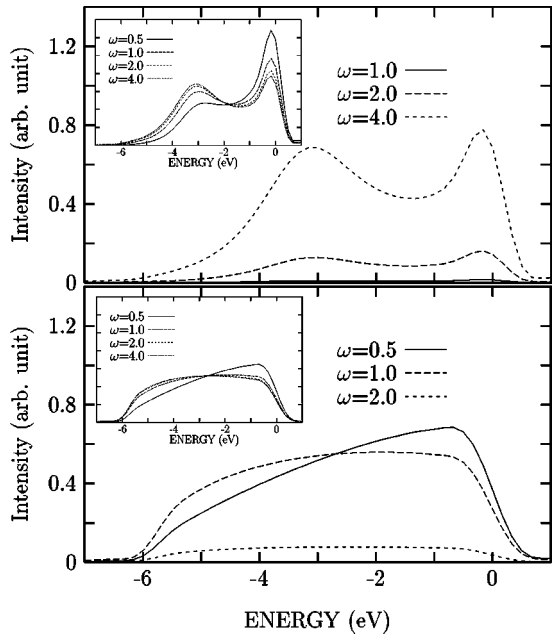

FIG. 4. The ω-dependent valence PES are given for $4f$ emission (upper panel) and $5d$ emission (lower panel). The spectra at $\omega=0.5$ in the upper panel or $\omega=4.0$ in the lower will be so tiny that they are not illustrated. In the respective inset, the spectra is normalized to have the same area to give the change of shape. The unit of ω is the atomic unit (1 a.u.$=$ 27.2 eV).

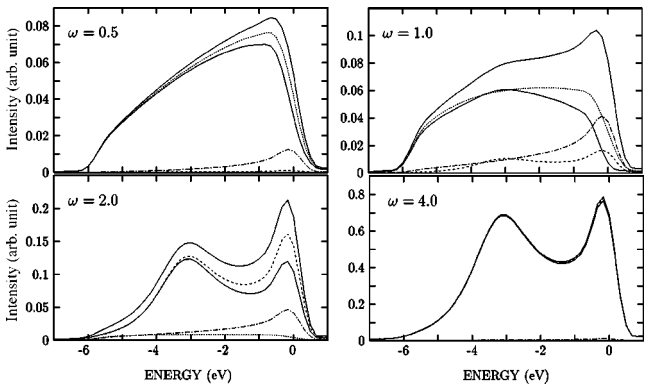

FIG. 5. The valence PES with respect to photon energies are provided. The relative strength of two channels is taken as $|\tilde{\Delta}_d/\tilde{\Delta}_f|=2.0$. Here two solid lines are the total spectra corresponding to constructive or destructive interference. The dashed line represents $4f$ emission, the dotted line $5d$ emission, and the dot-dashed line the interference contribution.

In Figs. 5 and 6, we see that at $\omega=0.5$ a.u., the dominant contributions are from $5d$-band emission because $\Delta_f(E)$ increases slowly compared to $\Delta_d(\epsilon,E)$, however, at $\omega=4.0$ a.u., most of the spectra in Ce arises from the $4f$ electrons because $\Delta_d(\epsilon,E)$ rapidly falls off over $E\sim 0.6$ a.u. Gunnarsson and Schönhammer[14] have obtained the total emission spectra involving the interference (of $4f$ and $5d$) based on the sudden approximation, but could not have discussed these behaviors with respect to ω. In the experiments, on the other hand, the increasing $4f$ and decreasing band features with varying ω has been used to separate the $4f$ structures.[13] That is, in the experiments, using He resonance lines, to subtract $\omega=0.78(=21.2$ eV) result from $\omega=1.5$ $(=40.8$ eV) result leads to approximately $4f$ emission for a moderate value of $|\tilde{\Delta}_d/\tilde{\Delta}_f|$ (i.e., say for $|\tilde{\Delta}_d/\tilde{\Delta}_f|\sim 2$).

Below, in Fig. 7, we can see the behaviors of interference as ω varies. As ω increases, the interference becomes stronger at first and then weaker again. That is, at about $\omega=1.0$ or 2.0 a.u., we see the strong interferences because both f and d emissions are comparable to each other, where the spectra

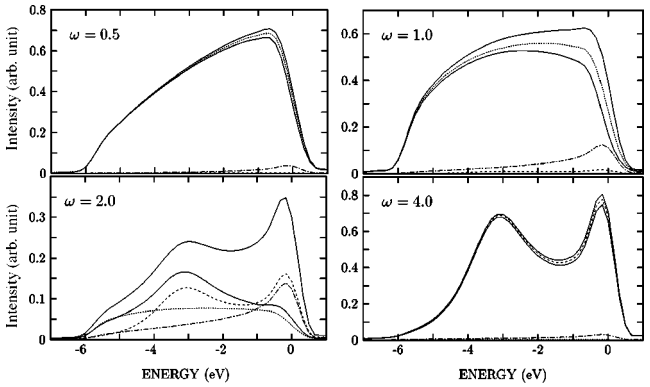

FIG. 6. The valence PES with respect to photon energies. The relative strength of two channels is taken as $|\tilde{\Delta}_d/\tilde{\Delta}_f|=6.0$. Notations are same as in Fig. 5.

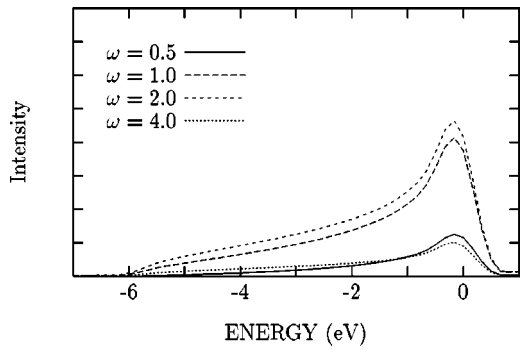

FIG. 7. The contributions of interference are given with respect to the photon energies. In the intermediate energies, the interferences are very strong.

cannot be understood from two separate emission spectra. Particularly in the case of strong destructive interference, although the $4f$ emission always comprises two peaks (see the inset of upper panel in Fig. 4), the peak near the Fermi level may be smeared in the total spectra.

V. LOW ENERGY VALENCE PHOTOEMISSION: EFFECTS OF PHOTOELECTRON SCATTERING

In the low photon energy region, we should consider the effects of photoelectron scattering potential induced by the hole left by the electron emission as well as the dipole matrix behavior. The band emission can also raise the shake-up effects such as plasmon satellites.[26] Nevertheless, in the present model, within $1/N_f$ expansion, the relevant bases of Eqs. (5)–(10) in the limit of $N_f \to \infty$ do not allow any conduction electron-hole excitation. Any shake-up behaviors from dielectric responses by band emissions then cannot be seen in the taken limit, but in the next higher order of $1/N_f$. For a hole in a localized f level, however, a small number of electrons may undergo measurable shifts in response to the potential induced by a hole.[27] For the photoelectron scattering potential, we should go back to Eq. (1) and see the interaction of a f-level impurity electron. In this section, we will confine our discussion only to the f-level valence photoemission, i.e., here we do not consider the interference with band contributions. In $\mathcal{H}(=\mathcal{H}_0+\Delta)$, it needs noting that the f-electron correlation is actually a quantity renormalized by the conduction electrons, that is,

$$U_{ff} n_f n_f + U_{fd} n_f \sum_\nu \int d\epsilon \psi^\dagger_{\epsilon\nu} \psi_{\epsilon\nu} = (U_{ff} - U_{fd}) n_f n_f = U n_f n_f, \tag{22}$$

where we have used $n_f + \Sigma_\nu \int d\epsilon \psi^\dagger_{\epsilon\nu} \psi_{\epsilon\nu}$ is a conserved quantity. In the similar way, we can compose the scattering potential term V_{SC} which must be added to $\mathcal{H}_0$

$$V_{\rm SC} = V_{4f}(\mathbf{r}) n_f + V_{5d}(\mathbf{r}) \sum_\nu \int d\epsilon \psi^\dagger_{\epsilon\nu} \psi_{\epsilon\nu} - V_{4f}(\mathbf{r}), \tag{23}$$

where it should be noted that the initial neutral (ground) state is $4f^1$. Then we have

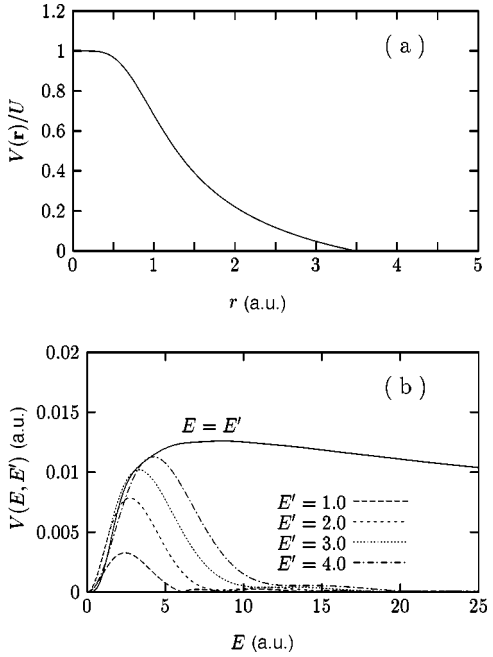

FIG. 8. (a) The photoelectron scattering potential $V(\mathbf{r})$ is given as normalized by U. (b) The diagonal and off-diagonal parts of scattering potential matrix are given.

$$V_{\rm SC} = [V_{4f}(\mathbf{r}) - V_{5d}(\mathbf{r})] n_f - V_{4f}(\mathbf{r}) = [V_{4f}(\mathbf{r}) - V_{5d}(\mathbf{r})](n_f - 1) - V_{5d}(\mathbf{r}). \tag{24}$$

We know $V_{5d}(\mathbf{r})$ is much broader and weaker than $V_{4f}(\mathbf{r})$ and better to be neglected. So we take $V_{\rm SC}$ as

$$V_{\rm SC} = V(\mathbf{r})(n_f - 1), \quad V(\mathbf{r}) = V_{4f}(\mathbf{r}) - V_{5d}(\mathbf{r}). \tag{25}$$

Then we cut off the potential by taking the muffin-tin radius r_{mt} as the radius of neutral Ce atom, $r_{mt} = 3.49$ a.u. $V_{4f}(\mathbf{r})$ and $V_{5d}(\mathbf{r})$ are evaluated from the Slater orbital. Now, $V(\mathbf{r})$ is a short range one due to a screening of conduction d electrons and have a simple relation between $V(\mathbf{r})$ and the intraatomic Coulomb correlation U,

$$U = \int d\mathbf{r} \rho_f(\mathbf{r}) V(\mathbf{r}) \approx V(0), \tag{26}$$

if we assume the f-level charge density $\rho_f(\mathbf{r})$ and the f level is quite localized like the core level. Thus $V(\mathbf{r})$ should be redefined by $(1/\varepsilon)V(\mathbf{r})$, where ε is a dielectric constant chosen to make sure of Eq. (26), being due to screening by the surrounding, so ε is $V(0)/U \approx 5.24$. The behavior of $V(\mathbf{r})$ is given in Fig. 8(a). Then we express the scattering potential in terms of the photoelectron basis function

$$V_{\rm SC} = \sum_\nu \int dE dE' V(E,E') \psi^\dagger_{E\nu} \psi_{E'\nu} \left[\sum_{\nu'} \psi^\dagger_{\nu'} \psi_{\nu'} - 1 \right], \tag{27}$$

where the potential matrix element $V(E,E')$ are

$$V(E,E') = \int d\mathbf{r} \varphi^*_{E\nu}(\mathbf{r}) V(\mathbf{r}) \varphi_{E'\nu}(\mathbf{r}). \tag{28}$$

As in calculating the dipole matrix, the photoelectron basis function $\varphi_{E\nu}(\mathbf{r})$ must be obtained by solving the Schrödinger

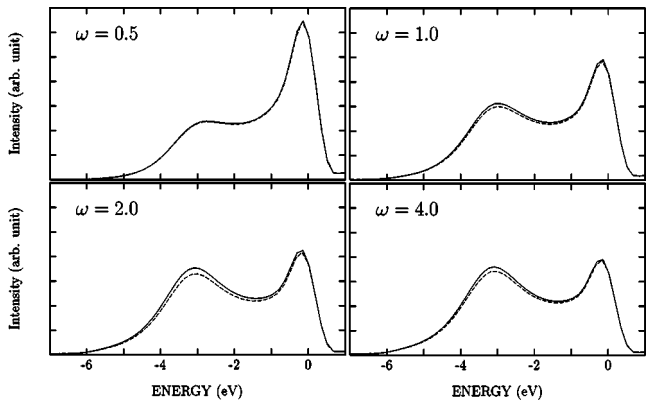

FIG. 9. Effects of scattering potential (solid line) are illustrated by comparing with noninteracting results (dashed line) at given photon energies.

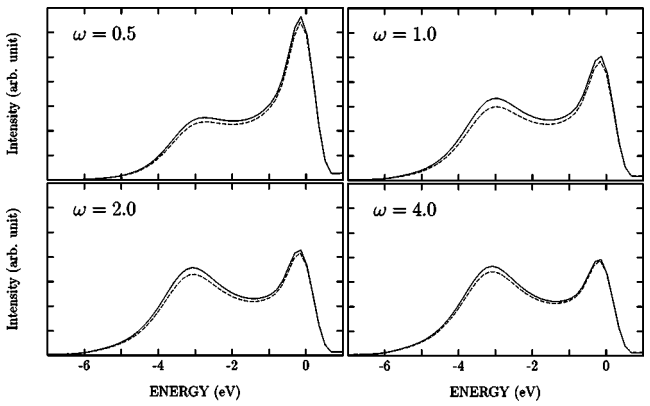

FIG. 10. Notations are same as in Fig. 9. Here the scattering potential range has been made a bit larger than in a Ce case, $r_{mt}=5.24$ a.u.

equation under the atomic potential. But here we use simple spherical Bessel function of $l=4$ as in the last section. We hopefully expect the essential feature will not be spoiled by neglecting the phase shift $\delta(k)$. So the desirable $\varphi_{E\nu}(\mathbf{r})$ is

$$\varphi_{E\nu}(\mathbf{r})=\frac{\sqrt{2}}{\sqrt{\pi}}(2E)^{1/4}j_4(\sqrt{2E}r)Y_{4m}(\hat{\mathbf{r}}) \tag{29}$$

and the matrix element $V(E,E')$ is

$$V(E,E')=\frac{2}{\pi}(4EE')^{1/4}\int drr^2 j_4(\sqrt{2E}r)V(r)j_4(\sqrt{2E'}r), \tag{30}$$

whose explicit behaviors are shown in Fig. 8(b).

As V_{SC} added, the total Hamiltonian $\mathcal{H}$ becomes $\mathcal{H}_0+\Delta+V_{\mathrm{SC}}$, corresponding to the extended AIM. Under $\mathcal{H}$, the valence PES via the f channel can be calculated. The comparison of the results with V_{SC} to those without V_{SC} (still including the dipole elements) is provided in Fig. 9. The effects of scattering potential are quite small as shown in Fig. 9, which must be due to a weak scattering potential in typical Ce compounds. Nevertheless, it is very meaningful to pursue a general consensus in the valence PES about the photoelectron scattering effects. In order to be more instructive, we also investigate the resulting behaviors for a slightly different potential whose range is a bit larger by 50% (see Fig. 10).

In both Figs. 9 and 10, it is notable that there are no appreciable changes in the peak near the Fermi level, while an increase in the ionization peak. This will be understood from the scattering potential $V(\mathbf{r})(n_f-1)$. The Fermi-level peak is from $4f^1\rightarrow 4f^1$, which will not be affected much by the potential because of $n_f=1$, but the ionization peak is from $4f^1\rightarrow 4f^0$. It is important to grasp the underlying physics from the spectral changes as the potential range is increased from $r_{mt}=3.49$ to $r_{mt}=5.24(1.5\times 3.49)$. Naturally a longer range potential results in more prominent effects in the spectra. In two respects, the spectral changes due to the photoelectron scattering look very similar to the core level PES in the ''shake down'' case in the previous work of ours.[16] First, if we simulate the absorption intensity ratio by the ratio of the ionization peak to the Fermi-level peak, we find the constructive interference between intrinsic and extrinsic processes in the low-energy regions just as in the shake down scenario of core level PES (the ratio is increased due to the scattering). The second point is the relevant energy scale governing the constructive interference due to the photoelectron scattering. In Fig. 9, we see the maximal scattering effects around $\omega\sim 2.0$, while, in Fig. 10, the energy scale giving the maximal effects is $\omega\sim 1.0$. That is, the governing energy scale is decreased by an increased range. In the core level PES, we found the relevant energy $(\tilde{E})$ can be directly related by the potential range $(\tilde{R})$ as $\tilde{E}=1/(2\tilde{R}^2)$, which tempts an application of the criteria to the present system. And it then can be a natural motivation that we make a parallel analysis for the adiabatic-sudden transition in this system and try to answer if the criteria found previously in core level PES can be still valid in this valence PES or not. This question is extensively discussed in the next section, where we propose the reduced two-level model for the sake of simplicity.

VI. ADIABATIC-SUDDEN TRANSITION FOR TWO-ELECTRON AND $N_f=2$

The AIM can be reduced into the two-level model, i.e., the whole continuum band is replaced by one level. The Hamiltonian $\mathcal{H}_0$ we should now consider is

$$\mathcal{H}_0=\epsilon_d\sum_\sigma \psi^\dagger_{d\sigma}\psi_{d\sigma}+\epsilon_f\sum_\sigma \psi^\dagger_{f\sigma}\psi_{f\sigma}$$
$$+V\sum_\sigma (\psi^\dagger_{f\sigma}\psi_{d\sigma}+\psi^\dagger_{d\sigma}\psi_{f\sigma})+Un_{f\uparrow}n_{f\downarrow}, \tag{31}$$

where $n_{f\sigma}=\psi^\dagger_{f\sigma}\psi_{f\sigma}$. Then the analogy of the present problem with the core level PES for the shake down case (having the ''level crossing'' as the hole is created) is more evident. The change of relevant electronic levels is given schematically before and after the photoemission in the following Fig. 11.

We can introduce three states $|f^0\rangle,|f^1\rangle$, and $|f^2\rangle$ as follows:

$$|f^0\rangle=\psi^\dagger_{d\uparrow}\psi^\dagger_{d\downarrow}|0\rangle,$$

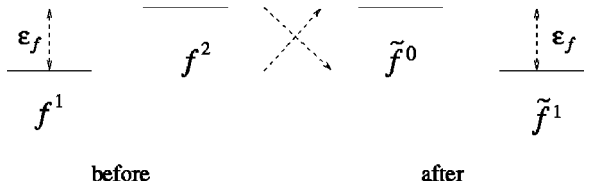

FIG. 11. Schematic view of the relevant configurations in initial and final stage. Here we assume $2\epsilon_f+U\approx 0$. Note there is a level crossing before and after the emission.

$$|f^1\rangle=\frac{1}{\sqrt{2}}[\psi^\dagger_{d\uparrow}\psi^\dagger_{f\downarrow}|0\rangle-\psi^\dagger_{d\downarrow}\psi^\dagger_{f\uparrow}|0\rangle],$$

$$|f^2\rangle=\psi^\dagger_{f\uparrow}\psi^\dagger_{f\downarrow}|0\rangle,$$

then we can express $\mathcal{H}_0$ in these bases,

$$\mathcal{H}_0=\begin{pmatrix} 0 & \overline{V} & 0 \\ \overline{V} & \Delta\epsilon & \overline{V} \\ 0 & \overline{V} & 2\Delta\epsilon+U \end{pmatrix}+2\epsilon_d, \tag{32}$$

where $\Delta\epsilon=\epsilon_f-\epsilon_d$ and $\overline{V}=\sqrt{2}V$. For simplicity, we will put $2\Delta\epsilon+U=0$. The ground state corresponding to the initial state of photoemission, $|\Psi_0\rangle$ is

$$|\Psi_0\rangle=\frac{\overline{V}}{\sqrt{\Delta_0^2+2\overline{V}^2}}[|f^0\rangle+\frac{\Delta_0}{\overline{V}}|f^1\rangle+|f^2\rangle], \tag{33}$$

where $\Delta_0=\frac{1}{2}\Delta\epsilon-\frac{1}{2}\sqrt{\Delta\epsilon^2+8\overline{V}^2}$ and its energy E_0 is

$$E_0=\Delta_0+2\epsilon_d. \tag{34}$$

The final states of the target are given by the following set of bases:

$$|\tilde{f}^0;\sigma\rangle=\psi^\dagger_{d\sigma}|0\rangle,$$

$$|\tilde{f}^1;\sigma\rangle=\psi^\dagger_{f\sigma}|0\rangle.$$

Then the Hamiltonian $\tilde{\mathcal{H}}_0$ with one f-electron emitted is

$$\tilde{\mathcal{H}}_0=\begin{pmatrix} 0 & \overline{V}/\sqrt{2} \\ \overline{V}/\sqrt{2} & \Delta\epsilon \end{pmatrix}+\epsilon_d. \tag{35}$$

Note $\psi_{f\sigma}|f^0\rangle=0$, $\psi_{f\sigma}|f^1\rangle=1/\sqrt{2}\sigma|\tilde{f}^0;-\sigma\rangle$, and $\psi_{f\sigma}|f^2\rangle=\sigma|\tilde{f}^1;-\sigma\rangle$ and σ is ± 1. Here σ is actually a redundant parameter. The possible final target states will be given by the eigenstates of $\tilde{\mathcal{H}}_0$ in Eq. (35),

$$|\Psi_1;\sigma\rangle=\cos\varphi|\tilde{f}^0;\sigma\rangle-\sin\varphi|\tilde{f}^1;\sigma\rangle, \tag{36}$$

$$|\Psi_2;\sigma\rangle=\sin\varphi|\tilde{f}^0;\sigma\rangle+\cos\varphi|\tilde{f}^1;\sigma\rangle, \tag{37}$$

where $E_{\frac{1}{2}}=\frac{1}{2}\Delta\epsilon\mp\frac{1}{2}\sqrt{\Delta\epsilon^2+2\overline{V}^2}+\epsilon_d(\delta E=\sqrt{\Delta\epsilon^2+2\overline{V}^2})$, and the parameter $\varphi(\pi/4<\varphi<\pi/2)$ is determined by

$$\tan\varphi=\frac{1}{\sqrt{2}}(\sqrt{w^2+2}-w),\quad w=\frac{\Delta\epsilon}{\overline{V}}. \tag{38}$$

Also noticeable is

$$\psi_{f\sigma}|\Psi_0\rangle=\frac{1}{\sqrt{2}}[-\sin\theta|\tilde{f}^0;-\sigma\rangle+\cos\theta|\tilde{f}^1;-\sigma\rangle], \tag{39}$$

where the parametric angle $\theta(\pi/4<\theta<\pi/2)$ is

$$\cot\theta=\frac{1}{2\sqrt{2}}(\sqrt{w^2+8}+w). \tag{40}$$

Now we consider the optical activation Hamiltonian Δ

$$\Delta=\sum_{k\sigma} M_k\psi^\dagger_{k\sigma}\psi_{f\sigma}. \tag{41}$$

Here it should be noted that we adopt the different photoelectron basis using k rather than E, i.e., having the normalization of $\delta_{kk'}$ than $\delta(E-E')$ [see Eqs. (17) and (18)], $\varphi_{k\sigma}(\mathbf{r})=(2/R)^{1/2}kj_4(kr)Y_{4m}(\hat{\mathbf{r}})$ (R: a big radius where the boundary condition is imposed), which could give an apparent analogy of the present simplified problem with the core level one. Within the first order perturbation theory, the photoemission matrix element $M(i,k\sigma)(i=1,2)$ will be

$$\begin{aligned} M(i,k\sigma) &= \left\langle \Psi_i;-\sigma\middle|\psi_{k\sigma}\left[1+V\frac{1}{E-\mathcal{H}_0-T+i\eta}\right]\Delta\middle|\Psi_0\right\rangle \\ &= m_iM_k+\sum_j c_{ij}m_j\sum_{k'}\frac{V_{kk'}M_{k'}}{\omega+E_0-E_j-\frac{1}{2}k'^2+i\eta}, \end{aligned} \tag{42}$$

where the scattering potential V_{SC} is taken as

$$V_{\mathrm{SC}}=V(\mathbf{r})(n_f-1),\quad V_{kk'}=\int d\mathbf{r}\varphi^*_{k\sigma}(\mathbf{r})V(\mathbf{r})\varphi_{k'\sigma}(\mathbf{r}) \tag{43}$$

and thus

$$m_i=\langle\Psi_i;-\sigma|\psi_{f\sigma}|\Psi_0\rangle,\quad c_{ij}=\langle\Psi_i;-\sigma|n_f|\Psi_j;-\sigma\rangle-\delta_{ij}.$$

That is, the coefficients are

$$m_1=-\frac{1}{\sqrt{2}}\sin(\varphi+\theta)\sigma,\quad m_2=\frac{1}{\sqrt{2}}\cos(\varphi+\theta)\sigma,$$

$$c_{11}=-\cos^2\varphi,\quad c_{22}=-\sin^2\varphi,\quad c_{12}=c_{21}=-\sin\varphi\cos\varphi.$$

If we consider a ratio between the main and the satellite absorption intensity divided by a noninteracting case $r(\omega)/r_0(\omega), r(\omega)/r_0(\omega)$ is

$$\frac{r(\omega)}{r_0(\omega)}=\left|\frac{1+\sin^2\varphi\,\frac{\tilde{V}}{\tilde{E}}F_{k_2}\left(\frac{\tilde{\omega}}{\tilde{E}}\right)-\frac{\sin 2\,\varphi\sin(\varphi+\theta)}{2\cos(\varphi+\theta)}\,\frac{\tilde{V}}{\tilde{E}}F_{k_2}\left(\frac{\tilde{\omega}+\delta E}{\tilde{E}}\right)}{1+\cos^2\varphi\,\frac{\tilde{V}}{\tilde{E}}F_{k_1}\left(\frac{\tilde{\omega}+\delta E}{\tilde{E}}\right)-\frac{\sin 2\varphi\cos(\varphi+\theta)}{2\sin(\varphi+\theta)}\,\frac{\tilde{V}}{\tilde{E}}F_{k_1}\left(\frac{\tilde{\omega}}{\tilde{E}}\right)}\right|^2, \tag{44}$$

where $k_{\frac{1}{2}}=\sqrt{2(\omega+E_0-E_{\frac{1}{2}})}$, $\tilde{\omega}=\omega-\omega_{\rm th}$($\omega_{\rm th}=E_2-E_0$ is threshold energy for the satellite), and we exploit the model matrix elements M_k and $V_{kk'}$ as used in the previous core level case,

$$\sum_{k'}\frac{V_{kk'}M_{k'}}{\epsilon-\epsilon_{k'}+i\eta}=-\frac{\tilde{V}}{\tilde{E}}M_kF_k(\epsilon/\tilde{E}), \tag{45}$$

$$F_k(\epsilon)=\frac{1}{\pi}\int_0^\infty\frac{x^{10}dx}{[1+x^5]^2[1+(\tilde{R}k-x)^2][x^2-\epsilon-i\eta]}, \tag{46}$$

$$M_k=\frac{(\tilde{R}k)^5}{1+(\tilde{R}k)^5}, \tag{47}$$

$$V_{kk'}=\frac{\tilde{V}\tilde{R}}{R}\,\frac{(\tilde{R}^2kk')^5}{[1+(\tilde{R}k)^5][1+(\tilde{R}k')^5][1+\tilde{R}^2(k-k')^2]}, \tag{48}$$

where $\tilde{R}$ is the characteristic length scale of the system directly related to the potential range and $\tilde{E}=1/2\tilde{R}^2$. Here it is found that from Eq. (44), $r(\omega)/r_0(\omega)$ can be written essentially in the same mathematics as in the core level case. In the following Fig. 12, we give the behaviors of $F(\epsilon)$.

Similarly to the core case, we always have an overshoot behavior in $r(\omega)/r_0(\omega)$ in the low-energy limit, when $\delta E=0$,

$$\frac{r(\omega_{\rm th})}{r_0(\omega_{\rm th})}=\left[\frac{1-F(0)\,\frac{\tilde{V}}{\tilde{E}}\,\frac{\sin\varphi\sin\theta}{\cos(\varphi+\theta)}}{1+F(0)\,\frac{\tilde{V}}{\tilde{E}}\,\frac{\cos\varphi\sin\theta}{\sin(\varphi+\theta)}}\right]^2>1, \tag{49}$$

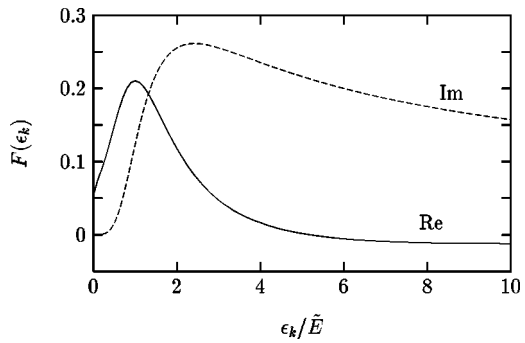

FIG. 12. The function $F(\epsilon_k)$ defined in Eq. (46). Both the real and imaginary parts are given.

where $F(0)=0.052286$ and $\pi/4<\varphi<\pi/2, \pi/4<\theta<\pi/2$, and $\pi/2<\varphi+\theta<\pi$ should be noted. In Fig. 13, we show $r(\omega)/r_0(\omega)$ as a function of $\tilde{\omega}/\tilde{E}$ for a few values of $\tilde{V}/\tilde{E}$.

Figure 13 shows as ω increases the ratio also increases and reaches a maximum. From the arguments in our previous work,[16] we see roughly $\tilde{R}\sim R_0/3$ and $\tilde{V}\sim 3V(0)/2$ and for Ce, $\tilde{R}\sim 1$ and $\tilde{V}\sim 0.3$, which leads to $\tilde{V}/\tilde{E}\sim 0.6$. Most notable is that the curves have the universal feature independent of $\tilde{V}/\tilde{E}$, i.e., the maximum positions are $\tilde{\omega}/\tilde{E}\sim 1$ and the overshoots disappear at about $\tilde{\omega}/\tilde{E}\sim 10$ irrespective of $\tilde{V}/\tilde{E}$. This means the adiabatic-sudden transition depends only on $\tilde{E}$, that is, $\tilde{R}$, even if the amplitude of overshoot relies on $\tilde{V}/\tilde{E}$. Beyond the first order perturbation, the overshoot range will be reduced due to the multiple scattering, but the universal behavior does not change. This conclusion is exactly identical to that in the core level case and implies the same criteria can be applied also to the valence PES case.

VII. CONCLUSION

We have studied the valence photoemission spectra in the Anderson impurity model aiming at Ce compounds. Using the time-dependent formulation and $1/N_f$ expansion, we can treat the problem exactly up to $\mathcal{O}(1/N_f)^0$. For Ce compounds, $N_f=\infty$ can be a good approximation for $N_f=14$. Within the formalism, to evaluate the photoemission spectra is corresponding to solving the time-dependent Schrödinger equation.

To investigate the low energy photoemission spectra, we should consider the dipole matrix and photoelectron scattering matrix additionally compared to the sudden approximation valid in high energy limit. In view of experiment, the valence PES always consist of *f* emission and band emission. So we considered both dipole matrix elements having explicit E dependencies and obtained the total spectra as well as two separate spectra with respect to the photon energies.

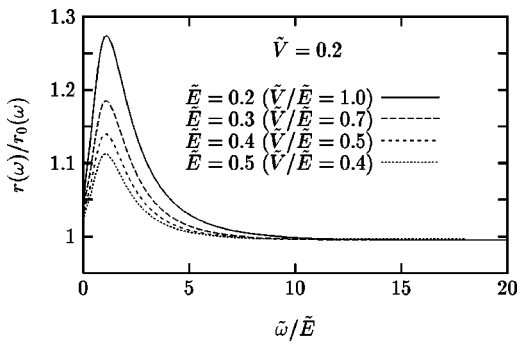

FIG. 13. The ratio $r(\omega)/r_0(\omega)$ as a function of $\tilde{\omega}/\tilde{E}$ for several values of $\tilde{V}/\tilde{E}$. $\Delta\epsilon/\overline{V}=-2.0$ is taken.

The relative strength and sign of two dipole elements are crucial in the total spectra. Due to differences in the energy scales of $4f$ and $5d$ dipole elements, the general trends are that, in a very low energy ($\omega \lesssim 1.0$ a.u.), the $5d$ emission is dominant, while the $4f$ emission increases and dominates over the $5d$ emission in a high energy ($\omega \gtrsim 2.0$ au). It is also found that the interference effects of f emission and band emission (from d) are highly nontrivial especially when the separate contributions are comparable to each other. Then (at $\omega \sim 1.0$ or 2.0 a.u., depending on the relative strength), due to a strong peak of the interferences near the Fermi level, the Kondo resonance peak of $4f$ emission may not be shown in the total spectra in the case of destructive interference. The constructive or destructive interference will be determined by the relative sign.

We also studied the effects of scattering potential for the f-electron emission. The model (AIM) is slightly extended to include the corresponding term. Scattering effects on the band emission is neglected in the infinite N_f limit. The potential matrix also includes the kinetic energy dependencies. It is a general result that in the case where the photoelectron couples to the localized excitation, the arrival at the sudden transition is much faster compared to the extended excitation. Extrinsic scattering gives the similar effects to the core level PES (Ref. 16) in the shake down case if we assign the Kondo resonance and ionization peak to the main and satellite peak, respectively. Its effects, however, are much smaller than in the core level case, which stems mainly from weaker potential strength and shorter range in Ce case. Nevertheless, interestingly, behaviors of two-peak ratio is reminiscent of the previous analysis of core level PES. Therefore, this can be a motivation to do a further analysis for the adiabatic-sudden behavior. We can then ask the question ''Can the criteria found in the core level case also be valid in the valence case.'' To explore this, first we simplify the model into just a two-level one, where the whole conduction band is replaced by one level. Then it is found the intensity ratio of two peaks can be written actually in the same way as in the core case. Through the same analysis, we can find that also in the valence PES, the sudden transition happens on the energy scale of $\tilde{E} = 1/(2\tilde{R}^2)$, where $\tilde{R}$ is a typical length scale of the scattering potential.

Finally, we would like to make it clear the scope or the outlook of our present model. Within the model, we cannot yet arrive at the realistic photoemission in a true solid. It is reported that the valence is altered at the surface, which gives important contributions to the photocurrent since the mean free path is quite small.[18,28] But it should be noted that the present PES study is based on $1/N_f$ expansion and $N_f \rightarrow \infty$ limit. In the $N_f \rightarrow \infty$ limit, the relevant excitation in the system is purely local, which is associated just with f and d occupation. This means the spectra are independent of the f-hole position. On the other hand, beyond the $N_f \rightarrow \infty$ limit, extended excitations from the conduction band start to enter the formalism. Beyond the limit we should in principle work in the generalized AIM including a term $\sim U'_{fd} n_f \Sigma_{\nu'} \int d\epsilon d\epsilon' \psi^\dagger_{\epsilon'\nu'} \psi_{\epsilon'\nu'}$ (no effects when $N_f \rightarrow \infty$), which raises the fluctuation potential for the photoelectron as $\sim V'(E,E';\epsilon,\epsilon') \psi^\dagger_{E\nu} \psi_{E'\nu} \psi^\dagger_{\epsilon'\nu'} \psi_{\epsilon'\nu'}$. Then the spectra become dependent on the f-hole position with respect to the surface[15] and the full spectra should be obtained by integrating the spectra over the f-hole position, where we may also consider the effects of valence altering near the surface by assuming $\epsilon_f(z)$ or $V(\epsilon;z)$ (z: f-hole position). Therefore, on the way to the full photoemission, we can naturally incorporate the surface effects in the spectra.

ACKNOWLEDGMENTS

The author would like to thank Lars Hedin, Olle Gunnarsson, and ByungIl Min for valuable discussions and their critical reading of the manuscript. The author is also grateful to Jim Allen for the useful information on recent Ce photoemission studies.

[1] P.W. Anderson, Phys. Rev. **124**, 41 (1961).
[2] A. Kotani, H. Mizuta, T. Jo, and J.C. Parlebas, Solid State Commun. **53**, 805 (1983); A. Kotani (unpublished), and references therein.
[3] J. Zaanen, C. Westra, and G.A. Sawatzky, Phys. Rev. B **33**, 8060 (1986).
[4] J.M. Lawrence, P.S. Riseborough, and R.D. Parks, Rep. Prog. Phys. **41**, 1 (1981); S. Hüfner and P. Steiner, Z. Phys. B: Condens. Matter **46**, 37 (1982); for a general reference, see J.W. Allen, S.J. Oh, O. Gunnarsson, K. Schönhammer, M.B. Maple, M.S. Torikachvili, and I. Lindau, Adv. Phys. **35**, 275 (1986); D. Malterre, M. Grioni, and Y. Baer, *ibid.* **45**, 299 (1996).
[5] C.-O. Almbladh and L. Hedin, in *Handbook on Synchrotron Radiation*, edited by E.-E. Koch (North-Holland, Amsterdam, 1983), Vol. 1B.
[6] O. Gunnarsson and K. Schönhammer, Phys. Rev. B **28**, 4315 (1983).
[7] J.W. Allen, S.-J. Oh, I. Lindau, J.M. Lawrence, L.I. Johansson, and S.B. Hagström, Phys. Rev. Lett. **46**, 1100 (1981).
[8] M. Croft, J.H. Weaver, D.J. Peterman, and A. Franciosi, Phys. Rev. Lett. **46**, 1104 (1981).
[9] N. Mårtensson, B. Riehl, and R.D. Parks, Solid State Commun. **41**, 573 (1982).
[10] D.J. Peterman, J.H. Weaver, and M. Croft, Phys. Rev. B **25**, 5530 (1982).
[11] D.M. Wieliczka, J.H. Weaver, D.W. Lynch, and C.G. Olson, Phys. Rev. B **26**, 6056 (1982).
[12] H. Sugawara, A. Kakizaki, I. Nagakura, T. Ishii, T. Komatsubara, and T. Kasuya, J. Phys. Soc. Jpn. **51**, 915 (1982).
[13] F. Patthey, B. Delley, W.-D. Schneider, and Y. Baer, Phys. Rev. Lett. **55**, 1518 (1985).
[14] O. Gunnarsson and K. Schönhammer, Phys. Rev. B **31**, 4815 (1985).
[15] L. Hedin, J. Michiels, and J. Inglesfield, Phys. Rev. B **58**, 15 565 (1998); J. Inglesfield, Solid State Commun. **40**, 467 (1981).
[16] J.D. Lee, O. Gunnarsson, and L. Hedin, Phys. Rev. B **60**, 8034 (1999).
[17] A.B. Andrews, J.J. Joyce, A.J. Arko, J.D. Thompson, J. Tang, J.M. Lawrence, and J.C. Hemminger, Phys. Rev. B **51**, 3277 (1995); H. Kumigashira, S.-H. Yang, T. Yokoya, A. Chainani, T. Takahashi, A. Uesawa, T. Suzuki, and O. Sakai, *ibid.* **54**,

9341 (1996); J.D. Denlinger, G.-H. Gweon, J.W. Allen, C.G. Olson, Y. Dalichaouch, B.-W. Lee, M.B. Maple, Z. Fisk, P.C. Canfield, and P.A. Armstrong (unpublished).

[18] J.W. Allen, G.-H. Gweon, H.T. Schek, L.Z. Liu, L.H. Tjeng, J.-H. Park, W.P. Ellis, C.T. Chen, O. Gunnarsson, O. Jepsen, O.K. Andersen, Y. Dalichaouch, and M.B. Maple (unpublished).

[19] This plausibility argument is not always justified, but successfully applicable to the low density Ce systems. The discussion about relations between impurity and periodic (lattice) cases can be found in R.M. Martin, Phys. Rev. Lett. **48**, 362 (1982).

[20] A. Bringer and H. Lustfeld, Z. Phys. B: Condens. Matter **28**, 213 (1977).

[21] O. Gunnarsson and K. Schönhammer, Phys. Rev. B **22**, 3710 (1980).

[22] J.F. Herbst and J.W. Wilkins, Phys. Rev. Lett. **43**, 1760 (1979).

[23] J.C. Slater, Phys. Rev. **36**, 57 (1930).

[24] S.H. Vosko, L. Wilk, and M. Nusair, Can. J. Phys. **58**, 1200 (1980).

[25] J.J. Yeh and I. Lindau, At. Data Nucl. Data Tables **32**, 1 (1985).

[26] F. Aryasetiawan, L. Hedin, and K. Karlsson, Phys. Rev. Lett. **77**, 2268 (1996).

[27] D.W. Lynch and J.H. Weaver, in *Handbook on the Physics and Chemistry of Rare Earths*, edited by K.A. Gschneider, Jr., L. Eyring, and S. Hüfner (North-Holland, Amsterdam, 1987), Vol. 10, and references therein.

[28] L.Z. Liu, J.W. Allen, O. Gunnarsson, N.E. Christensen, and O.K. Andersen, Phys. Rev. B **45**, 8934 (1992).